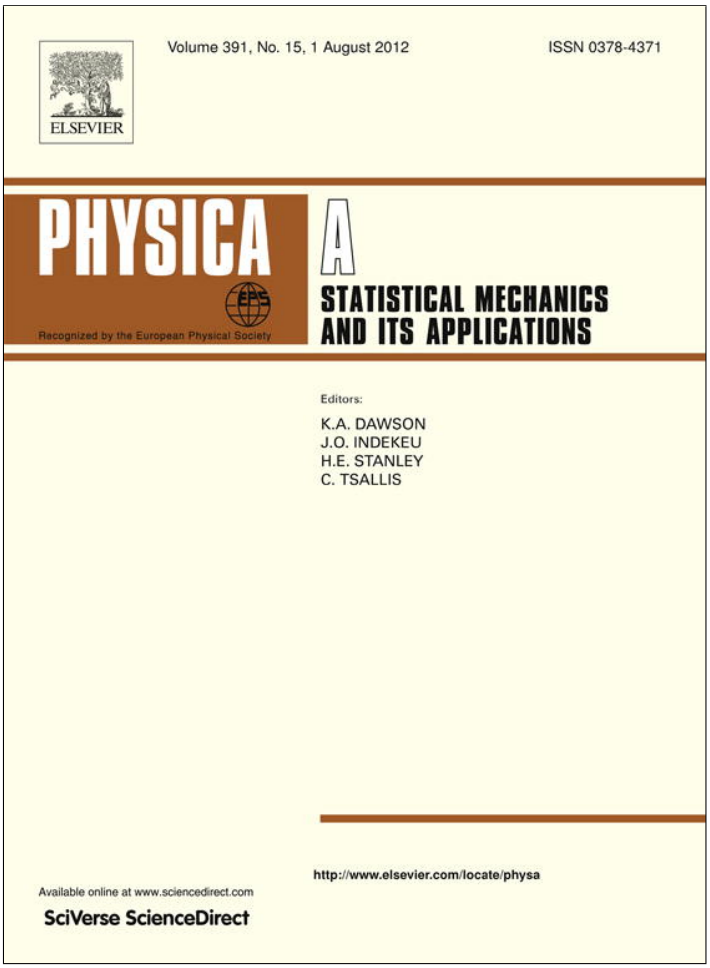

Physica A 391 (2012) 3797–3804

Contents lists available at SciVerse ScienceDirect

Physica A

journal homepage: www.elsevier.com/locate/physa

Thermal relaxation for the Relativistic Ornstein–Uhlenbeck Process

F. Debbasch [a,*], D. Espaze [a], V. Foulonneau [a], J.-P. Rivet [b]

[a] Université de Paris 6, ERGA-LERMA, UMR8112, 3 rue Galilée, F-94200 Ivry, France

[b] Université de Nice-Sophia Antipolis, CNRS, Observatoire de la Côte d'Azur, UMR6202, B.P. 4229, F-06304 Nice Cedex 04, France

ARTICLE INFO

Article history:
Received 28 December 2011
Received in revised form 16 February 2012
Available online 24 February 2012

Keywords:
Relativistic statistical physics
Diffusion

ABSTRACT

The thermal relaxation of a relativistic particle diffusing in a fluid at equilibrium is investigated through a numerical study of the Relativistic Ornstein–Uhlenbeck Process. The spectrum of the relaxation operator has both a discrete and a continuous component. Both components are fully characterized and the limit between them is given a simple interpretation. Short-time relaxation is addressed separately, and a global effective relaxation time is also computed. The general conclusion is that relativistic effects slow down thermalization.

1. Introduction

Transport at effectively bounded velocities occurs in a large variety of contexts, ranging from astrophysics [1] and fusion plasma physics [2,3] to metal [4,5] and computer engineering [6], and even tumor treatment [7,8]. Modeling such transport phenomena is a notoriously difficult problem [9–13]. The Relativistic Ornstein–Uhlenbeck Process (ROUP) has been introduced in 1997 [14] as the simplest possible model of relativistic particle transport and can also be used as a blueprint [13] to construct models of non relativistic transport at bounded velocities.

Consider a relativistic particle diffusing in the absence of gravity through a fluid in a state of thermodynamical equilibrium. The ROUP is built after the traditional, non relativistic Langevin equation [15], and splits the force acting on the diffusing particle into a deterministic and a stochastic contribution. The deterministic contribution is a friction force and the stochastic contribution is a Gaussian white noise in the rest frame of the fluid which surrounds the diffusing particle.

Of particular interest is the asymptotic behavior of the process in both position and momentum space. It has been shown in Ref. [16] by a standard Chapman–Enskog argument that the asymptotic behavior of the ROUP is described, in position space, by the usual diffusion equation. This has been confirmed in Ref. [17] by a more mathematically rigorous method. The ROUP also thermalizes the diffusing particle with the fluid by which it is surrounded [14]. The momentum space distribution of the ROUP thus tends towards a Jüttner distribution [18,19], which is the relativistic analogue of the equilibrium Maxwell distribution. The temperature of this Jüttner distribution coincides with the temperature of the fluid surrounding the diffusing particle.

Perhaps unexpectedly, the relaxation of the momentum distribution towards the equilibrium Jüttner distribution has never been studied in detail. This relaxation is entirely controlled by a linear differential operator $\mathcal{L}$ but very little detailed information is available about this operator. Previous publications [20,21] indeed offer bounds on the spectrum of $\mathcal{L}$ but do not determine if the spectrum is discrete or continuous, or how the eigenvalues depend on the physical parameters?

The aim of this article is to remedy this gap in the literature and to characterize as fully as possible the relativistic thermal relaxation of the ROUP. Here is a summary of our main results, which have all been obtained by numerical simulations in $(1+1)$ dimensions.

* Corresponding author. Tel.: +33 144277286; fax: +33 144277287.
E-mail address: fabrice.debbasch@gmail.com (F. Debbasch).

0378-4371/$ – see front matter
doi:10.1016/j.physa.2012.02.026

The operator $\mathcal{L}$ controlling the relaxation towards equilibrium depends on a single dimensionless quantity $Q = \sqrt{\frac{mc^2}{k_B\theta_e}}$, whose square is the ratio of the rest mass energy of the diffusing particle by the thermal energy at the equilibrium temperature θ_e (k_B is the Boltzmann constant). Since $\mathcal{L}$ describes a relaxation, its spectrum is non-positive. The Galilean regime corresponds to Q infinite; the operator $\mathcal{L}$ then coincides with the standard, non relativistic Ornstein–Uhlenbeck operator, which has a discrete spectrum [22]. We display numerical evidence that the spectrum is drastically different for finite values of Q *i.e.* in the relativistic regime. The spectrum of $\mathcal{L}$ then displays, not only a discrete component, but also a continuous component which lies below the discrete one. Moreover, all discrete eigenvalues seem to accumulate on the top of the continuous component as the coefficient Q tends to zero *i.e.* as the problem becomes more relativistic.

The operator $\mathcal{L}$ also has a finite spectral gap for all values of Q, and the inverse of this spectral gap is the asymptotic characteristic time of the thermalization process. The short-time relaxation, on the other hand, is best characterized by the slope of the temperature at the initial time $t = 0$; this slope depends, not only on Q but also on the initial conditions. Natural, physically relevant initial conditions are Jüttner distributions of various temperatures $\theta_i \neq \theta_e$. We find that the initial slope, at fixed initial temperature θ_i, increases as Q increases *i.e.* as the dynamics becomes more and more Galilean. At fixed Q, the slope decreases with the initial temperature θ_i.

The relaxation process can also be characterized by a series of intermediary characteristic times. We consider here the family of times τ_ϵ, defined as the times at which the temperature of the diffusing particle, which starts at θ_i and finishes asymptotically at θ_e, has reached the value θ_ϵ such that $\theta_\epsilon - \theta_i = (1-\epsilon)\,(\theta_e - \theta_i)$ These times also depend on Q and θ_i. Their typical dependance on these parameters is presented here on the particular case $\epsilon = 1/10$. The overall conclusion is that, at least in the model considered in this article, bounding velocities slows down thermalization.

2. The relativistic Ornstein–Uhlenbeck process (ROUP)

2.1. Presentation

This process describes the diffusion of a special relativistic point mass m in a fluid in a state of global equilibrium. It is completely defined, in n space dimensions, by the following set of stochastic differential equations, which are the equations of motion of the point mass in the rest frame of fluid:

$$\mathrm{d}\mathbf{x} = \frac{\mathbf{p}}{m\gamma}\mathrm{d}t \tag{1}$$

$$\mathrm{d}\mathbf{p} = -\alpha\frac{\mathbf{p}}{\gamma}\,\mathrm{d}t + \sqrt{2D}\,\mathrm{d}\mathbf{B}_t, \tag{2}$$

where $\gamma = \sqrt{1 + (\frac{\mathbf{p}}{mc})^2}$ and $\mathbf{p}^2$ is the squared Euclidean norm of $\mathbf{p}$. Eq. (1) is simply the definition of the relativistic n-momentum in terms of the velocity [23]. Eq. (2) states that the force acting on the particle splits into two contributions. The first one is a deterministic friction $-\alpha\mathbf{p}/\gamma$, which forces the n-momentum to relax to the vanishing n-momentum of the fluid in which the particle diffuses, and the second one is a n-dimensional centered Gaussian white noise. The associated Kolmogorov equation [14] reads:

$$\partial_t \Pi + \nabla_{\mathbf{x}} \cdot \left(\frac{\mathbf{p}}{\gamma m}\Pi\right) = \mathcal{L}_{\alpha,D}\,\Pi \tag{3}$$

where $\Pi(t, \mathbf{x}, \mathbf{p})$ is a density of the process with respect to the Lebesgue measure $\mathrm{d}^n x \mathrm{d}^n p$ in $\mathbb{R}^{2n}$ and $\mathcal{L}_{\alpha,D}$ is the relaxation operator:

$$\mathcal{L}_{\alpha,D}\,\Pi = \nabla_{\mathbf{p}} \cdot \left(\alpha\frac{\mathbf{p}}{\gamma}\,\Pi\right) + D\Delta_{\mathbf{p}}\Pi. \tag{4}$$

The marginal $f(t, \mathbf{p}) = \int_{\mathbb{R}^n} \Pi(t, \mathbf{x}, \mathbf{p})\mathrm{d}^n x$ obeys the simpler, relativistic Fokker–Planck equation:

$$\partial_t f = \mathcal{L}_{\alpha,D} f. \tag{5}$$

The process admits an invariant measure in momentum space [14]. The density $f^\star_{\alpha,D}$ of this measure with respect to $d^n p$ is the following stationary solution of (5):

$$f^\star_{\alpha,D}(\mathbf{p}) = a\,\exp\left(-\frac{\gamma\, m^2c^2\alpha}{D}\right), \tag{6}$$

where a is a normalization factor [14] such that $\int_{\mathbb{R}^n} f^\star_{\alpha,D}(\mathbf{p}) d^n p = 1$. This function is called a Jüttner distribution [18,19] and describes an equilibrium at temperature:

$$\theta_e = \frac{D}{k_B m\alpha}, \tag{7}$$

where k_B is the Boltzmann constant. This last equation is a fluctuation–dissipation relation for the ROUP.

The temperature $\theta(t)$ of the diffusing particle at time $t > 0$ is defined by Israel [10]:

$$\frac{n}{2}k_B\theta(t) = \left\langle \frac{\mathbf{p}^2}{2m\gamma} \right\rangle. \tag{8}$$

Here, $\langle\cdot\rangle$ denotes the expectation computed with the distribution f at time t.

Let us now introduce the following dimensionless variables:

$$T = \alpha t, \qquad \mathbf{P} = \sqrt{\frac{\alpha}{D}}\,\mathbf{p} = Q\frac{\mathbf{p}}{mc}. \tag{9}$$

In terms of the dimensionless variable $\mathbf{P}$, the Lorentz factor γ reads: $\Gamma_Q(\mathbf{P}) = \sqrt{1+(\mathbf{P}/Q)^2}$, where $Q = \sqrt{\frac{mc^2}{k_B\theta_e}}$. Note that the Galilean limit corresponds to $Q \to \infty$ (thermal energy small compared to mass energy).

The momentum-space density of the process, expressed as a function F of T and $\mathbf{P}$ then obeys the Fokker–Planck or forward Kolmogorov equation:

$$\partial_T F = \mathcal{L}_Q F = \nabla_{\mathbf{P}} \cdot \left(\frac{\mathbf{P}}{\Gamma_Q(\mathbf{P})} F \right) + \Delta_{\mathbf{P}} F. \tag{10}$$

The operator $\mathcal{L}_Q$ is the adjoint with respect to $\mathrm{d}\mathbf{P}$ of the generator of the diffusion in $\mathbf{P}$ space. The density $F_Q^\star$ of the invariant measure $\mathrm{d}\mu^\star$ with respect to d^nP takes the form:

$$F_Q^\star(\mathbf{P}) = A\,\exp\left(-Q^2\Gamma_Q(\mathbf{P})\right), \tag{11}$$

where A is a normalization factor.

The temperature ratio $\Theta(T) = \theta(T)/\theta_e$ is given by:

$$\frac{n}{2}\Theta(T) = \left\langle \frac{\mathbf{P}^2}{2\Gamma_Q(\mathbf{P})} \right\rangle, \tag{12}$$

where $\langle\cdot\rangle$ denotes the expectation computed with the distribution F at time T.

3. The spectrum of the relaxation operator $\mathcal{L}_Q$

To address this problem, we focus on the case $n = 1$ (one dimension in P space). Information about the spectrum of the relaxation operator $\mathcal{L}_Q$ can be obtained by integrating numerically the imaginary-time, Schrödinger-like equation:

$$\mathrm{i}\partial_T \Psi = \mathcal{L}_Q \Psi, \tag{13}$$

and Fourier-analyzing the temporal behavior of the solution Ψ. Indeed, assume a solution (13) can be expanded on eigenfunctions Ψ_λ of $\mathcal{L}_Q$ so that, for all T and P:

$$\Psi(T,P) = \Sigma_\lambda a_\lambda(T)\Psi_\lambda(P), \tag{14}$$

where the summation may be discrete or continuous. Plugging this expansion into (13) leads to

$$\mathrm{i}\frac{\mathrm{d}}{\mathrm{d}T}a_\lambda = \lambda a_\lambda \tag{15}$$

or

$$a_\lambda(T) = A_\lambda \exp(-\mathrm{i}\lambda T) \tag{16}$$

where the A_λ's are integration constants. The function Ψ is then a superposition of imaginary exponentials, the λ's are the frequencies of these exponentials and they can thus be recovered by Fourier-analyzing the time-dependence of Ψ.

This method for probing numerically the spectrum of an operator is not new and is used extensively in quantum chemistry; a traditional reference is [24]. As discussed below, the proper mathematical setting for all computations carried out in this article is a rigged Hilbert space; there are several approaches to eigenfunction expansions and spectral theorems in rigged Hilbert spaces; popular ones are discussed in Refs. [25–27].

The procedure just described has been implemented on Mathematica 8.0 with several initial and boundary conditions. Various numerical integration methods have also been tested. The numerical results are consistent with the following picture. For all finite values of Q, the spectrum of $\mathcal{L}_Q$ is real, negative and admits both a discrete and a continuous component. The discrete component is bounded from below by a critical value: $\lambda^c(Q) = -Q^2/4$ and the continuous component starts at $\lambda^c(Q)$ and does not seem to have a lower bound.

The graph in Fig. 1 displays the first four discrete eigenvalues of the spectrum, as a function of the Q factor. The parabola in dashed line represents the critical value $\lambda^c(Q) = -Q^2/4$. These results suggest that the discrete eigenvalues accumulate towards $-Q^2/4$ as Q decreases. If that is indeed the case, the spectral gap [21] of $\mathcal{L}_Q$ is equal, for all values of Q, to the first non vanishing eigenvalue, denoted by $\lambda_1(Q)$ in Fig. 1.

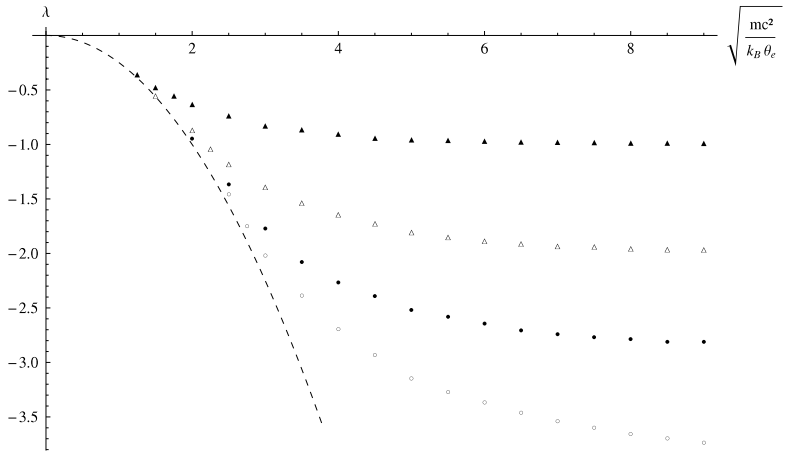

Fig. 1. The first four eigenvalues as a function of $Q = \sqrt{mc^2/k_B\theta_e}$. Solid triangles: λ_1; empty triangles: λ_2; solid circles: λ_3; empty circles: λ_4. The dashed line is the function $\lambda^c(Q) = -Q^2/4$, delimiting the discrete and continuous components of the spectrum.

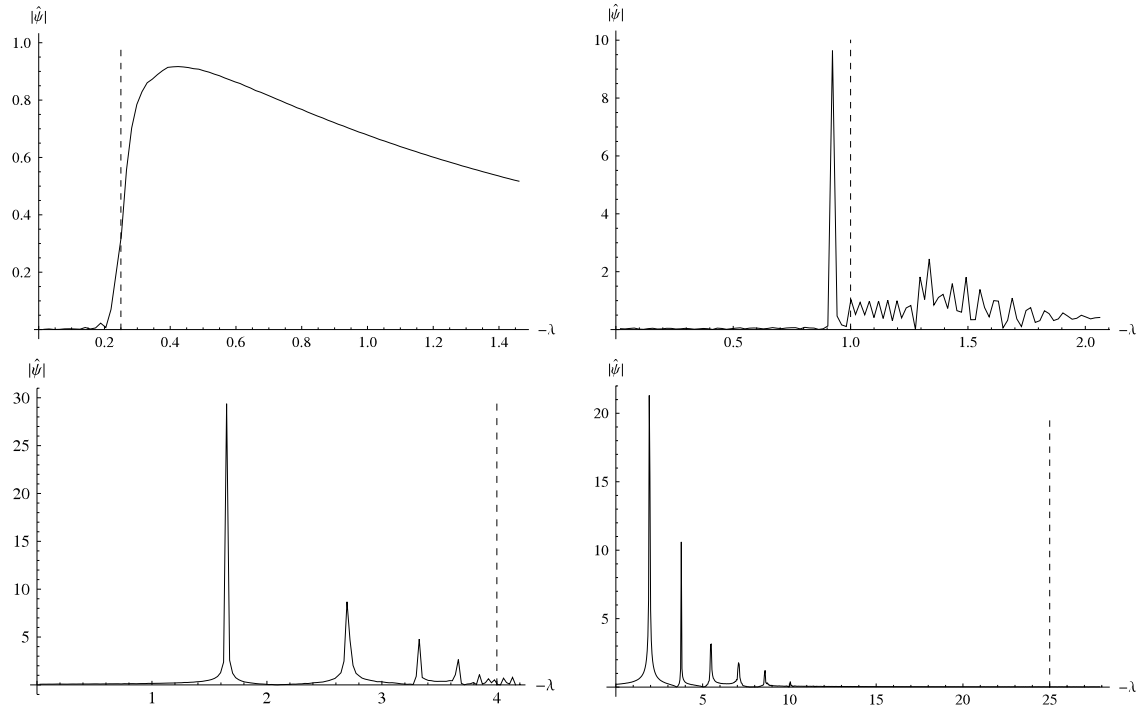

Fig. 2. Modulus of the time Fourier transform of even solutions of (13) for $Q = 1.0$ (top-left), $Q = 2.0$ (top-right), $Q = 4.0$ (bottom-left) and $Q = 10$ (bottom-right). The dashed line corresponds to $\lambda = \lambda^c(Q)$, which is the limit between the continuous and discrete parts of the spectrum.

Figs. 2 and 3 offer typical examples of spectra from which the above conclusions are derived. Fig. 2 presents spectra of even solutions of (13) for $Q = 1$, 2, 4 and 10, and Fig. 3 presents spectra of odd solutions. The dashed line represents the critical value $\lambda^c(Q) = -Q^2/4$. The clearly distinct spikes on the left of this line signal the discrete component of the spectrum of $\mathcal{L}$. On the other hand, the structures appearing on the right on the line, be they oscillatory or not, do not display clearly define spikes and signal the presence of a continuous spectrum component. This interpretation is strengthened by the following observation: by changing initial conditions or boundary conditions at fixed Q, the spikes on the left of the dashed line do not change position. On the contrary, the structures on the right of the line do change, sometimes drastically, and the maxima and minima (for oscillatory structures like those displayed for $Q = 2$ and $Q = 4$) change positions. For smaller values Q, such as $Q = 1$, the continuous spectrum component is very clearly displayed on the right of the dashed line, but no spikes are clearly visible on the left of the line. The spikes of the discrete spectrum get closer and closer to the line as Q decreases (see Fig. 1 and the discussion in the above paragraph). We thus interpret the apparent absence of spikes on the left of the dashed line, not as the absence of a discrete spectrum component, but as the presence of a discrete spectrum component too close to the limit of the continuous one to be resolved numerically.

To get the eigenvectors corresponding to the discrete spectrum component, the eigenvalue problem $\lambda F = \mathcal{L}_Q F$ has been solved numerically with the values of λ given by the spikes in the spectrum of the numerical solution of (13). The first four

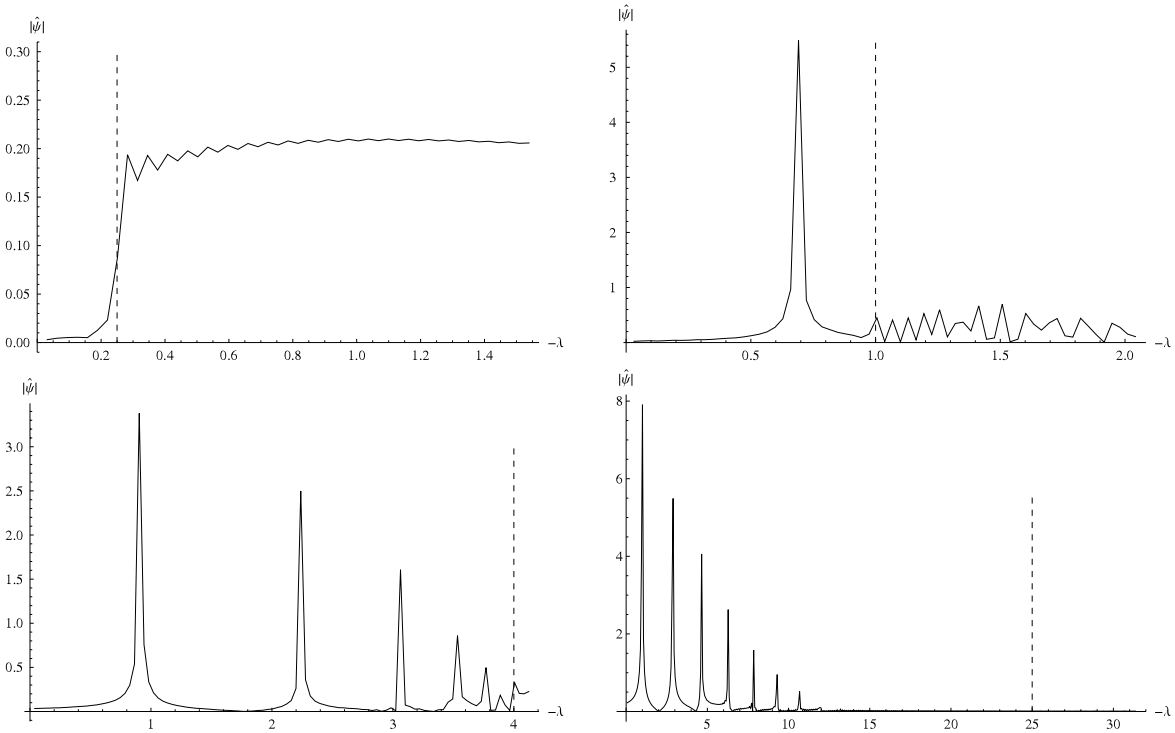

Fig. 3. Modulus of the time Fourier transform of odd solutions of (13) for $Q = 1.0$ (top-left), $Q = 2.0$ (top-right), $Q = 4.0$ (bottom-left) and $Q = 10$ (bottom-right). Here again, the dashed line corresponds to $\lambda = \lambda^c(Q)$, which is the limit between the continuous and discrete parts of the spectrum.

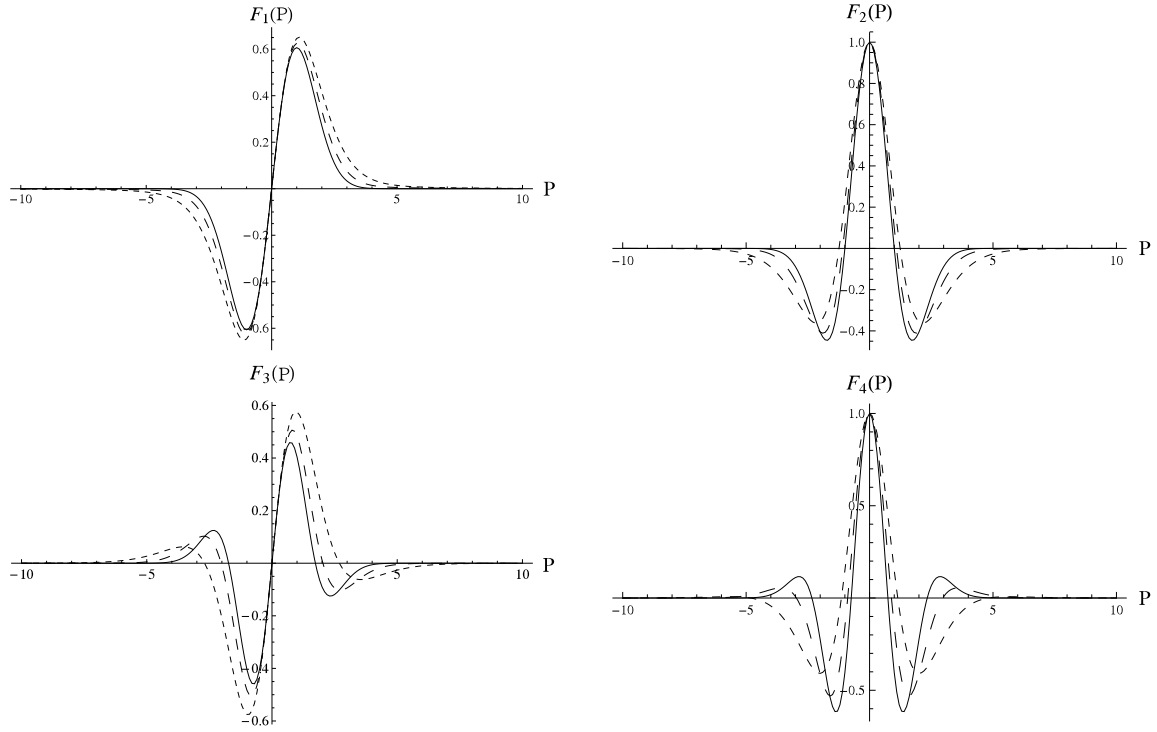

Fig. 4. The eigenvectors corresponding to λ_1 (top-left), λ_2 (top-right), λ_3 (bottom-left) and λ_4 (bottom-right), as a function of the momentum P, for the Galilean case (solid line), for $Q = 2.5$ (short-dashed line) and $Q = 4$ (long-dashed line).

eigenvectors are displayed in Fig. 4. The solid line corresponds to the Galilean limit ($Q \to \infty$). The short-dashed line and long-dashed line correspond respectively to $Q = 2.5$ and $Q = 4$.

The appearance of the continuous component of the spectrum at $\lambda^c(Q) = -Q^2/4$ can also be understood heuristically with the following reasoning. Consider the measure $\mathrm{d}\mu_Q = \mathrm{e}^{+Q^2\Gamma_Q(P)}\,\mathrm{d}P$ and the Hilbert space $\mathcal{H}(Q) = L^2(\mathrm{d}\mu_Q)$ containing all functions whose squared modulus can be summed against $\mathrm{d}\mu_Q$. This Hilbert space is equipped canonically with the

Hermitian product:

$$\langle F, G\rangle_Q = \int_{\mathbb{R}} F(P)\,\overline{G}(P)\mathrm{d}\mu_Q = \int_{\mathbb{R}} F(P)\,\overline{G}(P)\mathrm{e}^{Q^2\Gamma_Q(P)}\,\mathrm{d}P, \tag{17}$$

which makes the operator $\mathcal{L}_Q$ self-adjoint. Suppose now that F_λ is an eigenvector of $\mathcal{L}_Q$ with real eigenvalue λ. The asymptotic behavior of F_λ can be found heuristically by expanding the operator $\mathcal{L}_Q$ for $|P| \gg Q$. One thus finds that, asymptotically, F_λ obeys the following Fokker–Planck equation with constant coefficients:

$$\partial_{PP}F_\lambda + Q\epsilon(P)\partial_P F_\lambda = \lambda F_\lambda, \tag{18}$$

where $\epsilon(P)$ stands for the sign of P. Solutions of this equation are linear combinations of $E_{k_\pm}(P) = \exp(k_\pm P)$ with

$$k_\pm(\epsilon, Q) = \frac{-Q\epsilon \pm \delta}{2} \tag{19}$$

where $\delta^2 = Q^2 + 4\lambda$. The eigenfunction F_λ is in the Hilbert space $\mathcal{H}(Q)$ if it is square integrable against the measure $d\mu_Q$. According to (19), this is possible only if δ is real *i.e.* if $\lambda \geq \lambda^c(Q) = -Q^2/4$. Thus, eigenvectors associated to the discrete component of the spectrum do belong to $\mathcal{H}(Q)$ but those associated to the continuous spectrum component do not.

This situation is typical of continuous spectra, the simplest example being furnished by the usual Laplace operator. It is self-adjoint for the standard Hermitian product

$$\langle F, G\rangle = \int_{\mathbb{R}} F(P)\,\overline{G}(P)\mathrm{d}P, \tag{20}$$

defined in $L^2(\mathbb{R})$ (the Hilbert space of functions whose squared modulus can be integrated over $\mathbb{R}$ against $\mathrm{d}P$), but its spectrum is entirely continuous, the eigenfunctions being the imaginary exponentials, which are not in $L^2(\mathbb{R})$. Consider now the heat (or diffusion) equation with an initial condition in $L^2(\mathbb{R})$. The time-evolution of the solution can be found by expanding the initial condition on the eigenvectors of the Laplace operator *i.e.* by taking the spatial Fourier transform of the initial condition. This expansion is *not* the expansion of a function in $L^2(\mathbb{R})$ on a basis of $L^2(\mathbb{R})$, since the imaginary exponentials are *not* in $L^2(\mathbb{R})$. It does nevertheless furnish the correct solution to the heat equation and shows the role played by the continuous spectrum of the Laplace operator in building the time-evolution of the solution. The proper mathematical setting to develop the theory is not analysis in $L^2(\mathbb{R})$, but Schwartz distribution theory [28].

The same kind of conclusion applies to $\mathcal{L}_Q$; the spectrum of the operator has both a discrete and a continuous spectrum component; the eigenvectors of the discrete component are in $\mathcal{H}(Q)$, those of the continuous one are not, but both components contribute to thermalization process of the ROUP, even when the initial distribution is in $\mathcal{H}(Q)$. The proper mathematical setting which generalizes Schwartz distribution theory to operators other than the Laplace operator is not analysis in Hilbert spaces, but analysis in so-called rigged Hilbert spaces a.k.a. Gelfand triplets [25].

The Galilean case corresponds to $Q \to +\infty$; $\lambda^c(Q)$ is then also infinite and the standard Ornstein–Uhlenbeck relaxation operator $\mathcal{L}_\infty(F) = \partial_P(PF) + \partial_{PP}F$ thus has a pure point spectrum. It is indeed well-known that this point spectrum is made up of all negative integers $-\nu$ and that the eigenfunction associated to $-\nu$ is Hermite function $F_\nu(P) = H_\nu(P)\,\mathrm{e}^{-P^2/2}$, where H_ν is the ν-th Hermite polynomial [22].

Let us conclude this section by pointing out a final qualitative analogy, which has been suggested to us by one of the reviewers. Eq. (18) is formally identical, at least for positive values of P, to the equation of a mechanical damped harmonic oscillator[1]; F plays the role of the position, P plays the role of the time, Q is the friction coefficient and $-\lambda > 0$ is the squared pulsation of the oscillator. The discrete spectrum corresponds to λ's which make this oscillator overdamped, while the continuous spectrum corresponds to λ's which make this oscillator underdamped, in which case F displays oscillations as P tends to infinity. The Galilean regime is recovered as Q *i.e.* the friction coefficient tends to infinity. The oscillator is then overdamped for all values of the pulsation *i.e.* for all eigenvalues and the Galilean spectrum is thus purely discrete.

4. Further characterization of the relaxation

In order to compare the relaxation speed towards equilibrium for the Galilean and relativistic regimes, we have performed numerical integrations of the *real time* relativistic Fokker–Planck equation (10). We have chosen as initial condition a Jüttner distribution with arbitrary temperature θ_i.

4.1. Short-time relaxation

The short-time behavior of the relaxation can be characterized by the initial slope S_0 of the temperature evolution curve. This quantity has been computed for various values of the Q parameter, and for different temperature ratios θ_e/θ_i. Fig. 5 sums up these results. It displays the initial slope as a function of the temperature ratio for various values of Q. The solid line is the Galilean limit ($Q \to \infty$). The crosses correspond to $Q = 9$ and the solid circles to $Q = 1$.

[1] For negative values of P, Eq. (18) describes an oscillator damped in negative time.

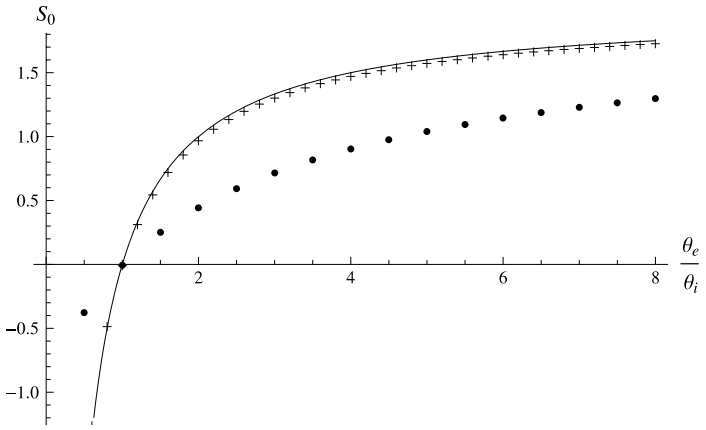

Fig. 5. The initial slope S_0 of the curve $\theta(T)$, as a function of the ratio θ_e/θ_i of the equilibrium temperature to the initial one, for the Galilean case (solid line), for $Q = 9$ (crosses) and $Q = 1$ (solid circles).

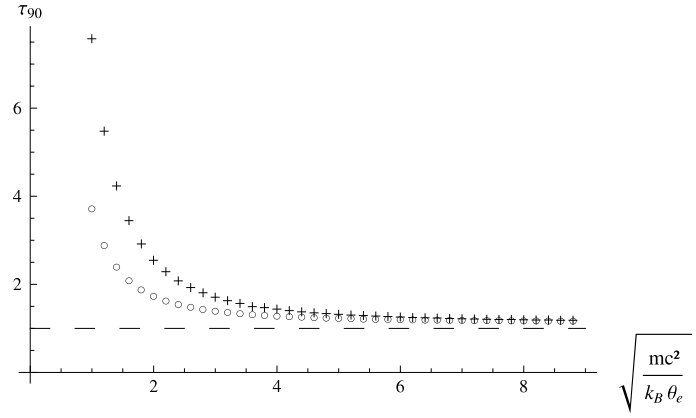

Fig. 6. The time τ_{90} for 90% relaxation, as a function of $Q = \sqrt{mc^2/k_B\theta_e}$, the cases $\theta_e/\theta_i = 0.5$ (crosses) and $\theta_e/\theta_i = 8$ (empty circles). The dashed line is the Galilean limit.

As expected, all curves reach the value 0 for $\theta_e/\theta_i = 1$ (there is then no evolution, since the initial temperature is equal to the equilibrium one). For any given value of θ_e/θ_i different from 1, the initial slope appears to be larger and larger as Q grows. Thus, initial relaxation seems faster in the unbounded velocity (Galilean) regime than in the bounded velocity (relativistic) one.

It is also worth noting that the initial slope curve is very close to its Galilean limit ($Q \to \infty$) for values of Q as low as 9 (curve with crosses).

4.2. Average global relaxation time

The initial slope of the temperature evolution curve contains only information about the short-time relaxation. To compare long-time relaxations, we have computed numerically the time τ_{90} needed for the initial temperature difference $\theta_e - \theta_i$ to be damped at 90%. This characteristic time has been plotted as a function of Q in Fig. 6, for two different temperature ratios ($\theta_e/\theta_i = 0.5$ for crosses, and $\theta_e/\theta_i = 8$ for empty circles).

The time τ_{90} decreases rapidly as $Q \to \infty$. This confirms that the relaxation process is slower in the bounded velocity (relativistic) regime than it is in the unbounded velocity (Galilean) one.

5. Conclusion

We have investigated the thermal relaxation of a relativistic particle diffusing in a fluid at equilibrium by performing numerical simulations of the $(1 + 1)$ Relativistic Ornstein–Uhlenbeck Process. The relaxation operator depends on a single parameter Q, whose square is the ratio of the rest-mass energy of the diffusing particle to its equilibrium thermal energy. We have found that the spectrum of the relaxation operator has both a discrete and a continuous component for all values of Q. We have investigated how the first discrete eigenvalues and the limit $\lambda_C(Q)$ between the discrete and continuous components of the spectrum depend on Q. We have also recovered the measured value of $\lambda_C(Q)$ through a simple analytical computation. We have finally characterized the short-time relaxation and defined a global effective relation time, which

has been computed for various values of Q and several initial conditions. The general conclusion is that, at least in the case considered in this article, bounding velocities slows down thermalization.

Let us now mention a few, natural extensions of this work. It would indeed be very interesting to study relativistic thermalization through other relativistic stochastic processes, notably the Dunkel–Haenggi process [29], and compare the results with those presented in this article. Since all relativistic processes also exist in curved space–time versions [30,20], one should also be able to investigate how a relativistic gravitational field influences thermalization. Relativistic momentum-space diffusion in the presence of a temperature or chemical potential gradient is another interesting problem, which could be addressed by using relativistic generalizations of the stochastic processes presented in Ref. [31]. Finally, all momentum-space studies should be seen as preludes to a full, detailed investigation of how relativistic stochastic processes behave in space–time.

Acknowledgment

This work has been funded by the grant no. ANR-09-BLAN-0364-01.

References

[1] P. Kumar, R. Narayan, MNRAS 395 (2009) 472–489.
[2] J. Martin-Solis, et al., Phys. Rev. Lett. 97 (2006) 165002.
[3] J. Freidberg, Plasma Physics and Fusion Energy, Cambridge, 2007.
[4] J. Klossika, U. Gratzke, M. Vicanek, G. Simon, Phys. Rev. B 54 (15) (1996) 10277–10279.
[5] T. Itina, M. Mamatkulov, M. Sentis, Opt. Eng. 44 (5) (2005) 051109–051116.
[6] H. Chen, J. Song, K. Liu, Jpn. J. Appl. Phys. 43 (7A) (2004) 4404–4410.
[7] K. Kim, Z. Guo, Comput. Methods Programs Biomed. 86 (2) (2007) 112–123.
[8] M. Jaunich, et al., Intl. J. Heat Mass Transfer 51 (2006) 5511–5521.
[9] C. Cattaneo, Atti Sem. Mat. Fis. Univ. Modena 3 (1948).
[10] W. Israel, in: A. Anile, Y. Choquet-Bruhat (Eds.), Relativistic Fluid Dynamics, in: Lecture Notes in Mathematics, vol. 1385, Springer-Verlag, Berlin, 1987.
[11] I. Müller, T. Ruggeri, Extended Thermodynamics, in: Springer Tracts in Natural Philosophy, vol. 37, Springer-Verlag, New-York, 1993.
[12] L. Herrera, D. Pavon, Phys. Rev. D 64 (2001) 088503.
[13] C. Chevalier, F. Debbasch, J. Rivet, Proceedings of the Second International Forum on Heat Transfer, IFHT08, Sept. 17–19, Tokyo, Japan, Heat Transfer Society of Japan, 2008.
[14] F. Debbasch, K. Mallick, J. Rivet, J. Stat. Phys. 88 (1997) 945.
[15] F. Reif, Fundamentals of Statistical and Thermal Physics, McGraw-Hill, Auckland, 1965.
[16] F. Debbasch, J. Rivet, J. Stat. Phys. 90 (1998) 1179.
[17] J. Angst, J. Franchi, J. Math. Phys. 48 (2007).
[18] F. Jüttner, Ann. Phys. (Leipzig) 34 (1911) 856.
[19] F. Debbasch, Physica A 387 (2008) 2443–2454.
[20] I. Bailleul, Annales de l'Inst. H. Poincaré 46 (2010) 760–795.
[21] J. Angst, JMP 52 (2011) 113703.
[22] A. Jeffrey, D. Zwillinger, Gradshteyn and Ryzhik's Table of Integrals, Series, and Products, Academic Press, 2007.
[23] L. Landau, E. Lifshitz, The Classical Theory of Fields, fourth ed., Pergamon Press, Oxford, 1975.
[24] M.D. Feit, J.A. Fleck, A. Steiger, J. Comp. Phys. 47 (1982) 412–433.
[25] K. Maurin, General eigenfunction expansions and group representations, Technical Report, 1966.
[26] F. Gomez-Cubillo, J. Phys. Conf. Series 128 (2008) 012039–012054.
[27] M. Gadella, F. Gomez-Cubillo, Acta. Appl. Math. 109 (2010) 721–742.
[28] I. Halperin, L. Schwartz, Introduction to the Theory of Distributions, University of Toronto Press, 1960.
[29] J. Dunkel, P. Hänngi, Phys. Rev. E 72 (2005) 036106.
[30] C. Chevalier, F. Debbasch, J. Math. Phys. 49 (2008) 043303.
[31] C. Chevalier, F. Debbasch, J. Rivet, Mod. Phys. Lett. B 23 (2009) 1147–1155.